

Effects of Phosphonate Herbicides on the Secretions of Plant-Beneficial Compounds by Two Plant Growth-Promoting Soil Bacteria: A Metabolomics Investigation

Wenting Li, Rebecca A. Wilkes, and Ludmilla Aristilde*

Cite This: *ACS Environ. Au* 2022, 2, 136–149

Read Online

ACCESS |



Metrics & More



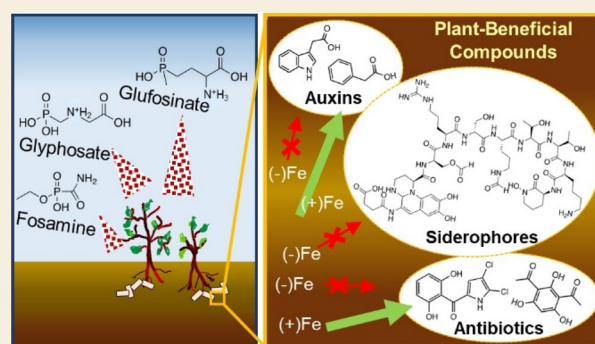
Article Recommendations



Supporting Information

ABSTRACT: Plant growth-promoting rhizobacteria (PGPR) that colonize plant roots produce a variety of plant-beneficial compounds, including plant-growth regulators, metal-scavenging compounds, and antibiotics against plant pathogens. Adverse effects of phosphonate herbicides, the most extensively used herbicides, on the growth and metabolism of PGPR species have been widely reported. However, the potential consequence of these effects on the biosynthesis and secretion of PGPR-derived beneficial compounds still remains to be investigated. Here, using high-resolution mass spectrometry and a metabolomics approach, we investigated both the intracellular metabolome and the extracellular secretions of biomass-normalized metabolite levels in two PGPR species (*Pseudomonas protegens* Pf-5, a Gram-negative bacterium; *Priestia megaterium* QM B1551, a Gram-positive bacterium) exposed to three common phosphonate herbicides (glyphosate, glufosinate, and fosamine; 0.1–1 mM) in either iron (Fe)-replete or Fe-deficient nutrient media. We quantified secreted auxin-type plant hormone compounds (phenylacetic acid and indole-3-acetic acid), iron-scavenging compounds or siderophores (pyoverdine and schizokinen), and antibiotics (2,4-diacetylphloroglucinol and pyoluteorin) produced by these PGPR species. The Fe-replete cells exposed to the phosphonate herbicides yielded up to a 25-fold increase in the production of both auxin and antibiotic compounds, indicating that herbicide exposure under Fe-replete conditions triggered metabolite secretions. However, the herbicide-exposed Fe-deficient cells exhibited a near 2-fold depletion in the secretion of these auxin and antibiotic compounds as well as a 77% decrease in siderophore production. Intracellular metabolomics analysis of the Fe-deficient cells further revealed metabolic perturbations in biosynthetic pathways consistent with the impaired production of the plant-beneficial compounds. Our findings implied that compromised cellular metabolism during nutrient deficiency may exacerbate the adverse effects of phosphonate herbicides on PGPR species.

KEYWORDS: Herbicide, Glyphosate, Glufosinate, Fosamine, Soil Bacteria, Metabolomics



INTRODUCTION

The application of phosphonate herbicides, which has reached an exponential trend in the United States (U.S.) over the past three decades,^{1,2} is critical to enhancing crop yield by controlling weeds.³ Among the most widely used phosphonate herbicides are glyphosate and glufosinate (Figure 1A).^{1,2} For instance, up to 1.0 kg ha⁻¹ of glyphosate was applied in 2014 on cultivated cropland in the U.S.;¹ more than 2.7 million kg of glufosinate was used to grow crops in the U.S. in 2017.⁴ Fosamine, another phosphonate herbicide, is primarily used to target woody plants,⁵ and around 1.6 thousand pounds of fosamine was applied to grow vegetables and fruits in the Washington State of the U.S. during 2016.⁵ The intensive use of phosphonate herbicides is of significant environmental concern due to their persistence in the environment, transportation through soil and water bodies, and toxicity to nontarget environmental organisms, including soil microorganisms.^{6–9} In recent years, plant growth-promoting

rhizobacteria (PGPR) have been increasingly applied as biofertilizers to enhance plant nutrient uptake or to act as plant disease control agents.^{10–14} Here, we sought to investigate the impact of phosphonate herbicides on two PGPR—*Pseudomonas protegens*¹⁵ (formerly known as *P. fluorescens*; a Gram-negative species) and *Priestia megaterium*¹⁶ (formerly known as *Bacillus megaterium*; a Gram-positive species).

These predominant PGPR species are currently used in agriculture^{17–21} and are known for their production of plant-

Received: September 1, 2021
Revised: October 24, 2021
Accepted: November 8, 2021
Published: November 18, 2021



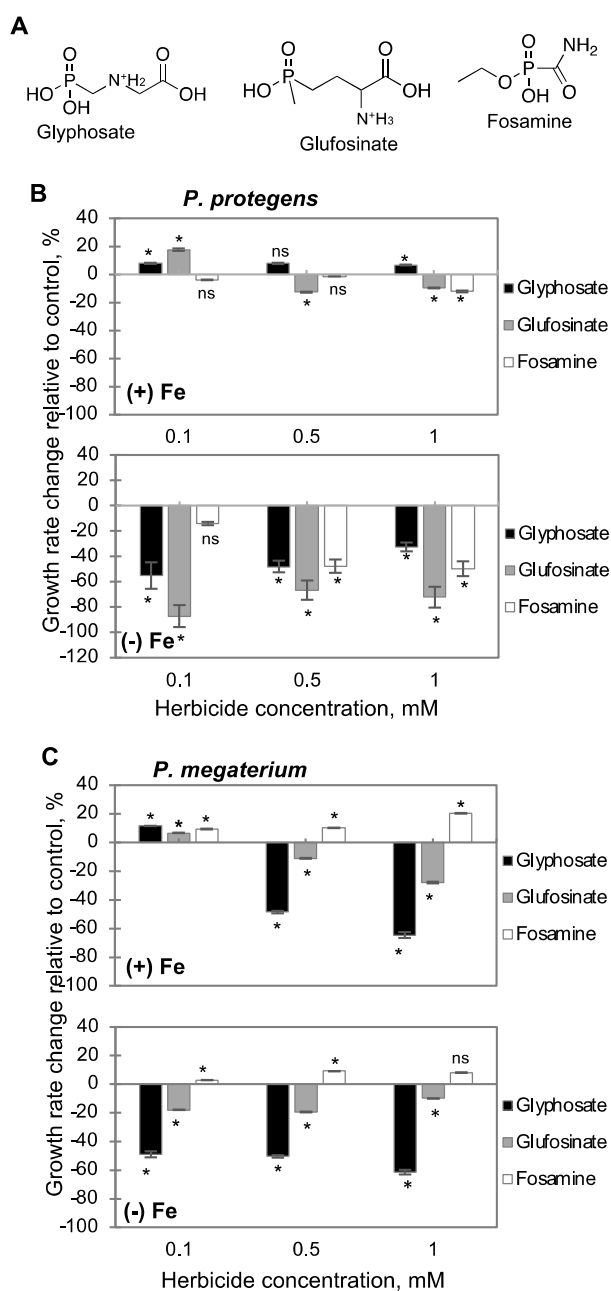


Figure 1. (A) Chemical structures of glyphosate, glufosinate, and fosamine. Relative effects of herbicide exposure on the specific growth rate of exponentially growing cells of (B) *P. protegens* and (C) *P. megaterium* grown under (top) Fe-replete [(+)Fe] and (bottom) Fe-limited [(-)Fe] conditions. Statistical analysis comparing the specific growth rates of cells grown in nutrient media without and with each herbicide at the specified concentration: *, $p < 0.05$; ns, not statistically significant.

beneficial compounds, such as plant hormones, iron-chelating compounds, and antibiotics.^{12–14} Cells of *P. protegens* and *P. megaterium* are known to secrete, respectively, the auxins phenylacetic acid²² and indole-3-acetic acid,²³ which are plant hormones known to regulate plant growth and development by controlling cell division, elongation, and differentiation.²⁴ Both species also secrete siderophores, which are strong iron-chelating compounds produced in response to iron deficiency, to facilitate iron acquisition by both bacteria and plants.²⁵ Specifically, *P. protegens* secretes the siderophore pyoverdine²⁶

and *P. megaterium* produces the siderophore schizokinen.²⁷ Due to the low bioavailability of iron in oxic soils²⁸ and the importance of iron for enzyme cofactors,²⁵ siderophore-secreting bacteria are essential to plant health.²⁵ Additionally, *P. protegens* is notable for the production of 2,4-diacetylphloroglucinol (DAPG)²⁹ and pyoluteorin,³⁰ two well-known antibiotics for antagonizing plant-pathogenic bacteria and fungi as well as suppressing plant diseases.³¹ Here, we aim to address to what extent the biosynthesis of these different beneficial compounds may be disrupted by exposure to each phosphonate herbicide (glyphosate, glufosinate, or fosamine) under varying doses in the bacterial nutrient media.

Previous studies have reported several adverse effects of phosphonate herbicides on PGPR.³² For instance, the population of PGPR species in the rhizosphere of glyphosate-resistant crops was shown to be diminished after glyphosate exposure.³³ Likewise, a decline in the growth rate or metabolic diversity of culturable soil bacteria³⁴ including *Pseudomonas* species,³⁵ was previously reported following exposure to glyphosate or glufosinate. However, the ability of various soil bacteria to degrade glyphosate^{36,37} and glufosinate³⁸ also implies that there are potential metabolic mechanisms that have evolved in soil bacteria to promote resilience to phosphonate herbicides.

The mode of toxic action of each phosphonate herbicide is an important consideration in investigating the metabolic responses of soil bacteria exposed to the herbicides. Whereas the mode of action of fosamine is not well understood,³⁹ the mode of action is well-known for glyphosate⁴⁰ and glufosinate.⁴¹ In both plants⁴⁰ and bacteria,⁴² glyphosate was found to inhibit the shikimate pathway, which involves seven steps to convert phosphoenolpyruvate (PEP) and erythrose-4-phosphate to chorismate,⁴³ a precursor to aromatic amino acids (i.e., phenylalanine, tyrosine, and tryptophan) and several secondary metabolites such as auxins.⁴³ It was determined that glyphosate disrupts the shikimate pathway in plants by inhibiting the 5-enolpyruvyl-shikimate-3-phosphate (EPSP) synthase, which catalyzes the reaction that combines shikimate-3-phosphate (S3P) and PEP to generate EPSP and inorganic phosphate.^{40,43} Recently, it was reported that glyphosate-exposed *Pseudomonas* species exhibited accumulation of S3P and depletion of aromatic amino acids, indicating the inhibition of the EPSP synthase in the shikimate pathway of these soil bacteria similar to plants.⁴²

The inhibition of the shikimate pathway responsible for the biosynthesis of aromatic amino acid pool could be consequential for the biosynthesis of the auxin phenylacetic acid derived from phenylalanine in *P. protegens*⁴⁴ and the auxin indole-3-acetic acid derived from tryptophan in *P. megaterium*.⁴⁵ Moreover, a previous study showed that glyphosate induced widespread perturbations in the metabolome of soil *Pseudomonas* species,⁴² which could further exacerbate effects on metabolic fluxes to siderophore biosynthesis. For instance, the biosynthesis of the pyoverdine siderophores in Fe-limited *P. protegens* requires chorismate from the shikimate pathway to produce the catecholate moiety and α -ketoglutarate [α -KG, a metabolite in the tricarboxylic acid (TCA) cycle] to produce the hydroxamate moiety in these siderophores.²⁶ Additionally, the biosynthetic pathway of pyoverdine incorporates PEP (a glycolysis metabolite), 3-phosphoglyceric acid (3-PG, another glycolysis metabolite), pyruvate (a glycolysis metabolite), and aspartate (an amino acid derived from the TCA cycle).²⁶ Likewise, the biosynthesis of the siderophore schizokinen in *P.*

megaterium relies on several metabolic precursors, such as aspartate and glutamate (two amino acids derived from TCA cycle intermediates), acetyl-CoA (a central carbon metabolite), and citrate (a metabolite in the TCA cycle).⁴⁶ Despite the importance of different metabolic pathways in sustaining the biosynthesis of both auxins and siderophores in PGPR species, the consequence of known metabolic effects of glyphosate on the production of these plant-beneficial compounds has not been investigated.

With respect to the mode of action of glufosinate in plants and bacteria, it was reported that phosphorylated glufosinate binds irreversibly to glutamine synthetase,^{41,47} thereby preventing the amination of glutamate to glutamine,⁴¹ thus leading to ammonia accumulation and subsequent adverse growth effects.⁴¹ Glutamate and glutamine both serve as precursors to numerous secondary metabolites. Specifically, for the antibiotic pyoluteorin produced by *P. protegens*,³⁰ the biosynthetic pathway starts with the amino acid proline derived from glutamate, which is a product of the amination of α -KG.^{48–50} By inhibiting glutamine synthetase, glufosinate can lead to the accumulation of glutamate, which may subsequently facilitate enhanced carbon flux for the production of pyoluteorin. In regards to DAPG, which is another antibiotic produced by *P. protegens*, its biosynthetic pathway involved with the conversion of malonyl-CoA (derived from acetyl-CoA⁵¹) to phloroglucinol, which can be directly acetylated into monoacetyl-phloroglucinol and eventually DAPG.⁴⁸ Interestingly, 2-chlorobenzene-1,3,5-triol (PG-Cl), which is derived from phloroglucinol in the DAPG biosynthetic pathway, was reported to be a metabolic coregulator that induced pyoluteorin production but suppressed DAPG production in *P. protegens*.⁴⁸ Therefore, metabolic effects on pyoluteorin biosynthesis may also affect the biosynthesis of DAPG in *P. protegens* cells.

Based on the aforementioned modes of action, we put forth three hypotheses regarding the mechanisms by which phosphonate herbicides can disrupt the biosynthesis of plant-beneficial compounds secreted by *P. protegens* and *P. megaterium*. First, we hypothesized that glyphosate would inhibit auxin production by interfering with the shikimate pathway and thus impair the biosynthesis of aromatic amino acid precursors to auxin biosynthesis. Second, we hypothesized that phosphonate herbicides would inhibit siderophore secretion that is reliant on central carbon metabolites in Fe-deficient cells by disrupting metabolic homeostasis. Third, we hypothesized that glufosinate would increase antibiotic production by inhibiting the glutamine synthetase pathway and thus increasing the flux of glutamate to pyoluteorin biosynthesis. To evaluate our stated hypotheses, we conducted a metabolomics investigation using high-resolution liquid chromatography–mass spectroscopy (LC-MS) to study the effects of each phosphonate herbicide (glyphosate, glufosinate, or fosamine) on the biosynthetic pathways and secretion of plant-beneficial compounds in *P. protegens* and *P. megaterium*, two relevant PGPR species. Due to the low solubility of Fe minerals in soils especially in oxic environments, wherein dissolved Fe species in the soil solution could be 4–5 orders of magnitude lower than what is required for biological cells, Fe is often a limiting nutrient to plants and soil microorganisms.⁵² Thus, at varying herbicide concentrations and under both Fe-replete and Fe-deficient conditions, we investigated the following: (1) cell biomass growth and substrate consumption, (2) extracellular biodegradation of each phosphonate herbi-

cide, (3) the intracellular metabolite levels in the biosynthetic pathways of the beneficial compounds, and (4) the extracellular secretions of auxin, siderophores, and antibiotics. Our findings provide new insights on the implications of phosphonate herbicide exposures in regards to the application of PGPR to benefit crops in agriculture.

MATERIALS AND METHODS

Materials

P. protegens Pf-5¹⁵ (formerly known as *P. fluorescens*) and *P. megaterium* QM B1551 *megaterium*¹⁶ (formerly known as *B. megaterium*) were obtained from ATCC (American Type Culture Collection, Manassas, VA). All the chemicals were obtained analytical grade from Sigma-Aldrich (St. Louis, MO, USA) and Fisher Scientific (Pittsburgh, PA, USA), except for glufosinate ammonium (Alfa Aesar, Ward Hill, MA, USA) and fosamine ammonium (Chemservice, West Chester, PA).

Culturing Conditions

Cell cultures (three biological replicates) were grown at 30 °C in a Thermo Scientific SHKE6000-7 incubator shaker (Thermo Fisher Scientific Waltham, MA) at 220 rpm.^{53,54} The growth medium, which was pH-adjusted (pH 7.0) and filter-sterilized (0.22 μ m nylon; MilliporeSigma, Darmstadt, Germany), contained the following major salts: 20 mM K₂HPO₄, 5 mM NaH₂PO₄, 0.81 mM MgSO₄·7H₂O, 37 mM NH₄Cl, 17.1 mM NaCl, 34 μ M CaCl₂·2H₂O. The trace metal concentrations were as follows: 0.96 μ M CuSO₄·5H₂O, 0.97 μ M H₃BO₃, 9.5 μ M ZnSO₄·7H₂O, 0.87 μ M MnSO₄·5H₂O, 0.21 μ M NiCl₂·6H₂O, and 0.34 μ M Na₂MoO₄·5H₂O. Succinate (200 mM C)⁵³ was provided as the carbon source for *P. protegens* Pf-5, and glucose (55 mM C)⁵⁴ was provided as the carbon source for *P. megaterium* QM B1551. The cells were grown under iron (Fe)-replete conditions with 30 μ M total dissolved unchelated Fe or under Fe-deficient conditions with 50 nM total dissolved unchelated Fe. For the Fe-deficient conditions, Fe concentrations were buffered by using disodium ethylene-diamine-tetra-acetic-acid (EDTA) as a strong iron chelator. The cells were subjected to different concentrations (0.1, 0.5, or 1 mM) of the three phosphonate herbicides (glyphosate, glufosinate, or fosamine) added to the nutrient medium described above—these concentrations were chosen to be within the concentration range (0.003–5 mM) used in previous studies.^{32,42,53,55} For our negative control conditions, the Fe-replete or Fe-limited nutrient media only contained the main carbon source (and nutrient salts as listed above) and no herbicide was added. The cells were transferred twice in the nutrient medium to make sure the cells were adapted to the medium composition under each condition. The growth curves were acquired by measuring the optical density at 600 nm using an Agilent Cary UV–visible spectrophotometer (Santa Clara, CA). Growth rates (h⁻¹) of exponentially growing cells were determined through regression analysis.

Extracellular and Intracellular Sampling

Extracellular Sampling. We harvested 1.5 mL samples of cell suspensions (three biological replicates) during the different phases of cell growth: at the beginning of the lag phase, at the early exponential growth phase, at the midexponential growth phase, and at the onset of stationary phase and at the stationary phase. Following centrifugation, at 10 000g for 5 min at 4 °C [Centrifuge 5423 R (Eppendorf, Hauppauge, NY)], we monitored the concentration of the main carbon substrate (succinate or glucose), herbicide (glyphosate, glufosinate, or fosamine), and species-specific plant beneficial compounds secreted by the cells. Dilution ratios of 1:100 or 1:1000 dilution with Milli-Q water (Fisher Scientific, Pittsburgh, PA) were conducted before analysis via LC-MS depending on the concentration of the extracellular metabolites.

Intracellular Sampling. For measuring the intracellular metabolites, exponentially growing cell suspensions were filtered [diameter of 47 mm, 22- μ m filters (Fisher Scientific, Waltham, MA)] and the cell-containing filters were immediately quenched by submerging

them in a cold ($-20\text{ }^{\circ}\text{C}$) 2 mL solution of methanol:acetonitrile:water (40:40:20). Solutions with the lysed cells were subsequently centrifuged at 10 000g for 5 min at $4\text{ }^{\circ}\text{C}$ (Centrifuge 5423 R, Eppendorf, Hauppauge, NY). Aliquots of 100 μL supernatants were dried under nitrogen gas and resuspended in 100 μL Milli-Q water (Fisher Scientific, Pittsburgh, PA) before analysis via high-resolution LC-MS. Metabolite levels were normalized to cell biomass quantity at the time of sampling.

Metabolomics and Compound Analyses via High-Resolution LC-MS

All analyses were conducted using reversed-phase ion-pairing ultrahigh performance liquid chromatography (Thermo Scientific Vanquish UHPLC) coupled with a high-resolution/accurate-mass spectrometer (Thermo Scientific Orbitrap Fusion Lumos Tribrid mass spectrometer) with electrospray ionization operated in negative mode. For the different analyses, we used C_{18} columns of different sizes for the liquid chromatography separation as detailed below. The metabolite identification via mass spectroscopy was based on high-precision of m/z , as validated by standards.

Metabolite Analysis. For the extracellular and intracellular metabolite extracts, we used a 10- μL injection sample and the column temperature was set to $25\text{ }^{\circ}\text{C}$. A 1.7- μm Waters Acquity UPLC BEH C_{18} column, with a size of $2.1 \times 100\text{ mm}$ (Waters Corporation, Massachusetts) was used. Solvent A contained 97:3 (v:v) LC-MS grade water:methanol with acetic acid (15 mM) and tributylamine (10 mM). Solvent B contained 100% methanol. The flow rate was $180\text{ }\mu\text{L min}^{-1}$ during the entire sample run (25 min). The solvent gradient with respect to solvent A was the following: 0 min, 100%; 2.5 min, 100%; 5 min, 80%; 7.5 min, 80%; 10 min, 45%; 12 min, 45%; 14 min, 5%; 17 min, 5%; 18 min, 0%; 25 min, 0%.⁴² The different compounds were identified based on their exact m/z values: S3P, $m/z = 253.0119$, retention time (r.t.) = 12.72 min; phenylalanine, $m/z = 164.0717$, r.t. = 4.21 min; tyrosine, $m/z = 180.0666$, r.t. = 2.36 min; glutamate, $m/z = 146.0459$, r.t. = 4.52 min; acetyl-CoA, $m/z = 808.1185$, r.t. = 14.38 min; α -KG, $m/z = 145.0143$, r.t. = 12.68 min; citrate, $m/z = 191.0197$, r.t. = 12.92 min; PEP, $m/z = 166.9751$, r.t. = 12.95 min; 3-PG, $m/z = 184.9857$, r.t. = 12.79 min; aspartate, $m/z = 132.0303$, r.t. = 4.64 min; and pyruvate, $m/z = 87.0088$, r.t. = 8.81 min.

Carbon Substrate Analysis. Succinate ($m/z = 117.0193$, r.t. = 11.49 min) was measured in the extracellular sample extracts using the method described above for metabolite analysis. The analytical method for extracellular glucose ($m/z = 179.0561$, r.t. = 7.15 min) was adapted from Liu et al.⁵⁶ We used a 3.5- μm XBridge BEH Amide column with a size of $2.1 \times 100\text{ mm}$ (Waters Corporation, Massachusetts). The flow rate was $150\text{ }\mu\text{L min}^{-1}$ during the entire sample run (13 min). The solvent gradient contained mobile phase A composed of 20 mM ammonium acetate and 15 mM ammonium hydroxide in LC-MS-grade water with 3% acetonitrile, prepared at pH 9.0; mobile phase B was 100% acetonitrile. The linear gradient used was as follows: 0 min, 85% B; 1.5 min, 85% B, 5.5 min, 35% B; 10 min, 35% B, 10.5 min, 85% B, 12.5 min, 85% B. Samples were prepared in 50% acetonitrile, and the injection volume was 5 μL . The concentration of each primary carbon substrate (glucose or succinate) was quantified with standards. Total substrate consumption was evaluated by comparing the substrate concentrations between the lag phase and the stationary phase of the cell growth.

Herbicide Analysis. To measure extracellular glyphosate ($m/z = 169.0140$, r.t. = 1.94 min), we used a cartridge holder with a column size of 30 mm \times 4.6 mm (Bio-Rad Laboratories, Hercules, CA) to process a solvent gradient containing 80% mobile phase A (0.1% formic acid in LC-MS grade water) and 20% mobile phase B (100% acetonitrile) during the 20 min run.⁵⁷ The injection sample was 50 μL , and the flow rate was 0.5 mL min^{-1} ; the column temperature was set to $40\text{ }^{\circ}\text{C}$. Extracellular glufosinate ($m/z = 180.0431$, r.t. = 7.97 min) was measured with the method described above for glucose measurement. Fosamine ($m/z = 152.0118$, r.t. = 8.32 min) was measured in the extracellular sample extracts using the method described above for metabolite analysis.

Analysis of Plant-Beneficial Compounds. The method for analyzing the plant beneficial compounds was developed based on a previous method by Xie et al.⁵⁸ We used a 5- μm A ZORBAX Eclipse Plus C_{18} column with the size of $4.6 \times 100\text{ mm}$ (Agilent Technologies, Santa Clara, CA, USA). The mobile phase A contained 100% acetonitrile. The mobile phase B contained 0.1% acetic acid in LC-MS grade H_2O . The flow rate was the following: 0 min, 0.5 mL/min; 9.0 min, 0.5 mL/min; 9.1 min, 1 mL/min; 13.2 min, 1 mL/min; 13.3 min, 0.5 mL/min. The solvent gradient with respect to solvent A was the following: 0 min, 30%; 2.1 min, 45%; 9 min, 100%; 11.2 min, 30%. The different compounds were identified based on their exact m/z values: phloroglucinol, $m/z = 125.0234$, r.t. = 2.45 min; 2-chlorobenzene-1,3,5-triol, $m/z = 158.9854$, r.t. = 2.23 min; phenylacetic acid, $m/z = 135.0452$, r.t. = 5.60 min; pyoluteorin, $m/z = 269.9736$, r.t. = 6.21 min; DAPG, $m/z = 209.0449$, r.t. = 7.73 min; and indole-3-acetic acid, $m/z = 174.0560$, r.t. = 5.15 min.

Siderophore Quantitation

Siderophore quantification for *P. protegens* Pf-5 was carried out in pH-adjusted (pH 7) bacterial supernatants (diluted if necessary) and was measured the absorbance at 400 nm using an Agilent Cary UV-visible spectrophotometer (Santa Clara, CA). A standard calibration curve was acquired with a PVD standard isolated from a *P. fluorescens* strain.²⁶ The Chrome Azurol S (CAS) method was used to quantify the schizokinen siderophore produced by *P. megaterium*.⁵⁹ Diluted extracellular supernatants were mixed with CAS assay solution,⁵⁹ followed by equilibrating for 5 h in the dark at room temperature. Mix solution was measured the absorbance at 630 nm using an Agilent Cary UV-visible spectrophotometer (Santa Clara, CA). Zero absorbance was measured with 50% CAS assay solution and 50% 0.1 mM desferrioxamine mesylate salt solution. A standard calibration curve was acquired with A/A_{ref} as a function of siderophore concentration, where A refers to the absorbance of desferrioxamine mesylate salt standard solution and A_{ref} is the reference absorbance. Reference absorbance was measured with MQ water. Reported siderophore production was normalized by the biomass quantity at the time of sampling.

Protein Sequence Similarity

The basic local alignment search tool (BLAST) was used to evaluate the similarity between two protein sequences. Two protein sequences were aligned with the tool protein-protein BLAST. The value of percent identity was used to evaluate the sequence identity between two proteins. The protein sequences involved in this study were available in the UniProt Knowledgebase (<https://www.uniprot.org/>). Specifically, we compared an EPSP synthase from the plant *Arabidopsis thaliana* (P05466) with two EPSP synthases from *P. protegens* Pf-5 (Q4K8N1, Q4K7P7) and two EPSP synthases from *P. megaterium* QM B1551 (D5DW56, D5DRE6). We also compared four glutamine synthetases from a wheat species *Triticum aestivum* (Q45NB2, Q45NB6, Q45NB7, Q6RUJ0) with one glutamine synthetase from *P. protegens* Pf-5 (Q4KJQ3) and one glutamine synthetase from *P. megaterium* QM B1551 (D5DQ10).

Statistical Analysis

All experiments were conducted in three biological replicates. Unpaired two-tailed t test analyses were conducted to evaluate statistically significant differences between two conditions (<https://www.graphpad.com/quickcalcs/ttest1/?format=SD>). Statistically significant difference was determined at $p < 0.05$.

RESULTS

Species-Specific and Herbicide-Specific Responses to Phosphonate Herbicide Exposure under Fe-Replete Conditions

For the fosamine-exposed Fe-replete cells, there were no adverse growth effects on *P. megaterium* at the varying doses (0.1–1 mM) or *P. protegens* cells at 0.1 and 0.5 mM doses, except for the growth of *P. protegens* at the highest fosamine

dose (1 mM) that was negatively affected (by ~12%) (Figure 1B,C). For glufosinate, the Fe-replete cells of both species did not exhibit appreciable adverse growth effects at 0.1 mM glufosinate, but the 1 mM glufosinate dose led to 10% and 30% decrease in the growth rates for Fe-replete *P. protegens* and *P. megaterium* cells, respectively, relative to control (Figure 1B,C). In response to exposure to glyphosate (up to 1 mM), there was a slight increase (up to 12%) in the specific growth rate for Fe-replete *P. protegens* Pf-5 cells but the growth rate of Fe-replete *P. megaterium* cells was reduced by up to 66% (Figure 1B,C). In sum, these data indicated that, whereas there were minimal growth effects of phosphonate herbicides on Fe-replete *P. protegens* cells, there were adverse growth effects on the Fe-replete *P. megaterium* cells with higher susceptibility to glufosinate and glyphosate than fosamine relative to control (Figure 1B,C). From monitoring extracellular concentration of each herbicide throughout the biomass growth, the lack of appreciable depletion in extracellular herbicide concentration led us to conclude that significant assimilation of degraded herbicides by *P. megaterium* cells was not involved in the observed enhanced growth rates [Appendices A–C, Supporting Information (SI)].

To determine whether inhibition of substrate uptake contributed to adverse growth effects, we also monitored the consumption of the main carbon substrate (i.e., succinate for *P. protegens* or glucose for *P. megaterium*) (Figure 2). Remarkably, despite the fact that the Fe-replete *P. megaterium* cells exhibited the most severe adverse growth effects, there was no change in their consumption of the carbon substrate when the cells were exposed to the herbicides across all concentrations, relative to control ($p \geq 0.141$) (Figure 2B). However, substrate consumption by the glyphosate-exposed Fe-replete *P. protegens* cells was inhibited by 8–26%, indicating that glyphosate exposure impeded the substrate uptake in Fe-replete *P. protegens* cells (Figure 2A). However, this inhibition did not cause adverse effects on the growth of *P. protegens* cells as previously discussed (Figure 1B). In the presence of glufosinate, there was no appreciable inhibition on the substrate consumption at 0.1 mM dose ($p = 0.079$), but a decrease by 6% and 22% in Fe-replete *P. protegens* cells at 0.5 and 1 mM glufosinate doses, respectively, implied that inhibition of substrate uptake contributed to the decreased growth rates of glufosinate-exposed Fe-replete *P. protegens* cells (Figure 2A). With respect to the fosamine-exposed Fe-replete cells, there was no appreciable difference in substrate consumption in the *P. protegens* cells ($p \geq 0.089$) (Figure 2A). Collectively, except for the *P. protegens* cells exposed to greater than 0.5 mM glufosinate, our data revealed that the adverse effects of phosphonate herbicides on the growth of the Fe-replete cells of both species were not related to the inhibition of the substrate uptake.

Iron-Deficiency Exacerbates Adverse Growth Effects of Phosphonate Herbicide Exposure on Both *P. megaterium* and *P. protegens*

Similar to the Fe-replete cells, fosamine exposure had no adverse effects on the growth rate of the Fe-deficient *P. megaterium* cells (Figure 1C). By contrast, the specific growth rate of Fe-deficient *P. protegens* cells was decreased by up to 52–55% at 0.5–1 mM fosamine doses, relative to control, compared to no change in Fe-replete *P. protegens* cells exposed to the same fosamine doses (Figure 1B). Whereas 0.1 mM dose of glufosinate did not negatively affect the biomass

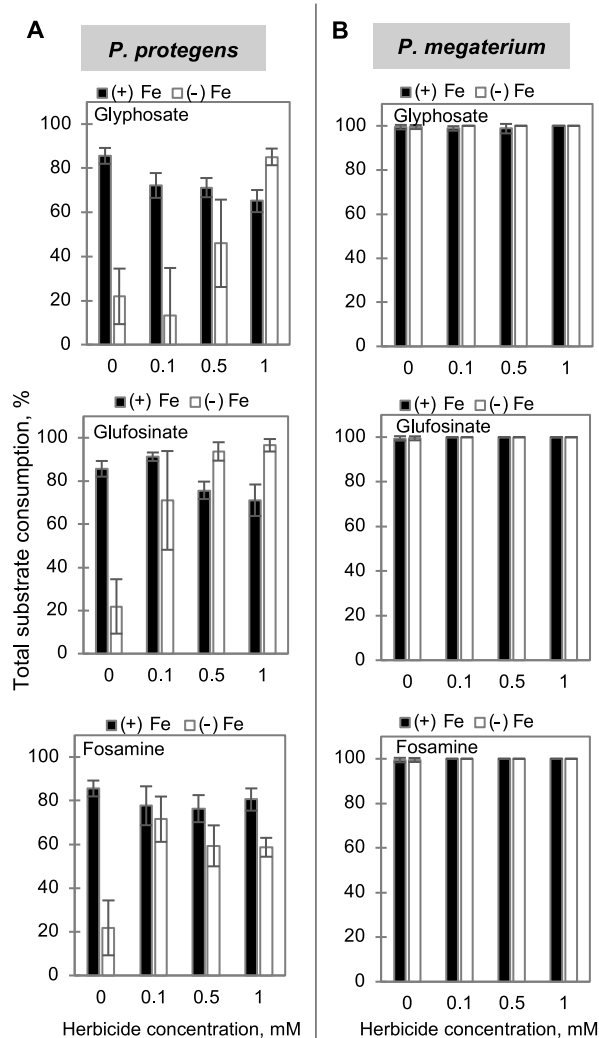


Figure 2. Total substrate consumption of (A) *P. protegens* and (B) *P. megaterium* cells exposed to (top) glyphosate, (middle) glufosinate, and (bottom) fosamine under Fe-replete (black) and Fe-limited (white) conditions under (top) Fe-replete [(+)Fe] and (bottom) Fe-limited [(-)Fe] conditions.

growth in the Fe-replete cells, Fe-deficient *P. protegens* and *P. megaterium* cells exhibited up to a 96% and 18% decrease, respectively, in specific growth rate at 0.1 mM dose of glufosinate (Figure 1B,C). At the highest glufosinate dose (1 mM), the specific growth rate of Fe-replete *P. protegens* and *P. megaterium* cells was decreased by up to 80% and 10%, respectively (Figure 1B,C). Compared to the less than 12% change in the specific growth rate of Fe-replete *P. protegens* exposed to glyphosate, the specific growth rate of Fe-deficient *P. protegens* cells was decreased by 32–65% across the three glyphosate doses (Figure 1B). For the Fe-deficient *P. megaterium* cells at the 0.1 mM glyphosate dose, the specific growth rate was decreased by up to 51%, compared to 11% for the Fe-replete cells (Figure 1C). At the highest glyphosate dose, the specific growth rates were comparable for Fe-replete and Fe-deficient *P. megaterium* cells (Figure 1C). In summary, our results highlighted that iron deficiency exacerbated the adverse growth effects on both *P. protegens* and *P. megaterium* cells exposed to the different phosphonate herbicides, except for Fe-deficient *P. megaterium* exposed to fosamine.

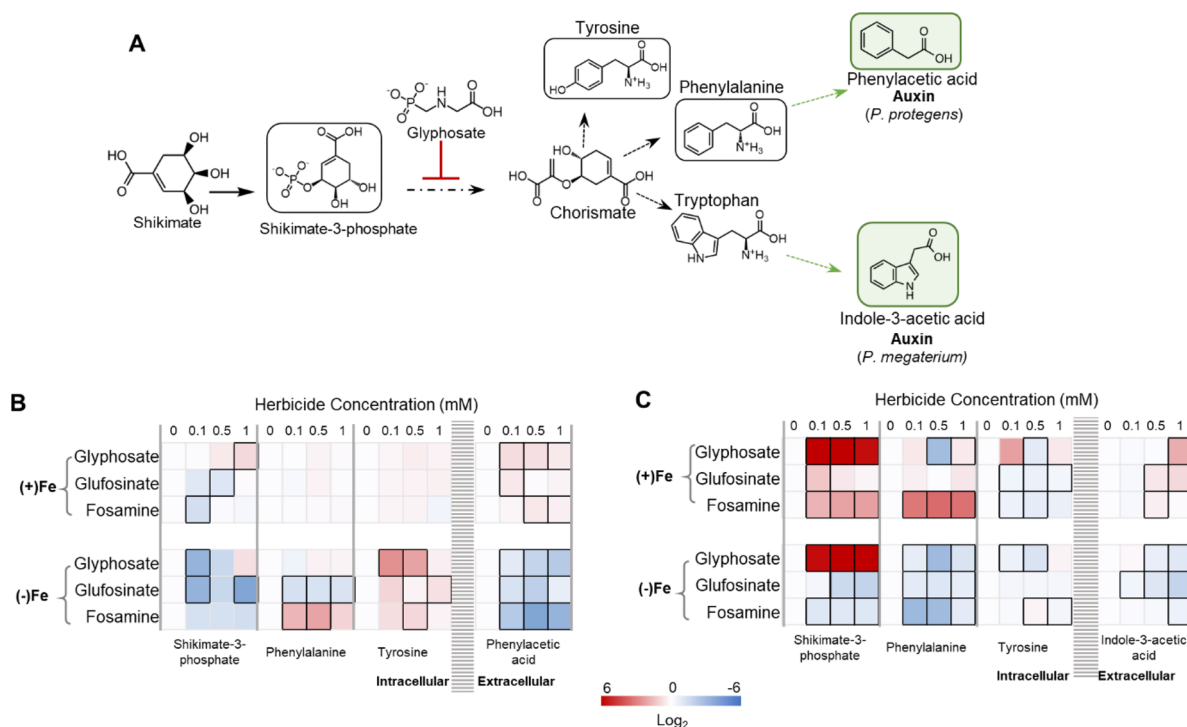


Figure 3. (A) Biosynthetic pathways of aromatic amino acids and auxin compounds in bacteria. Effects of herbicide exposure on the production of auxin compounds in (B) *P. protegens* and (C) *P. megaterium* cells under (top) Fe-replete [(+)Fe] and (bottom) Fe-limited [(-)Fe] conditions. In the reaction scheme in A, the measured metabolites are boxed: metabolite precursors (white); auxin compounds (green). Solid and dashed arrows refer to the occurrence of one reaction versus multiple reactions, respectively, between two metabolites. In B and C, all data are shown relative to control and statistically significant differences (calculated from unpaired two-tailed *t* test analyses, $p < 0.05$) are indicated by a black border.

Regarding the substrate uptake in Fe-deficient cells, we obtained substrate consumption in Fe-deficient *P. megaterium* cells that was comparable to that of control during the exposure to all three phosphonate herbicides ($p \geq 0.375$), indicating that the inhibition of the substrate uptake was likely not the cause of the adverse effects of glyphosate and glufosinate on the specific growth rate of Fe-deficient *P. megaterium* cells (Figure 2B). For Fe-deficient *P. protegens* cells exposed to phosphonate herbicides, there was a 4–78% increase in substrate consumption relative to control except for the 0.1 mM glyphosate dose, implying that the adverse growth effects of phosphonate herbicides on Fe-deficient *P. protegens* cells were not due to the impaired substrate uptake (Figure 2A). Furthermore, a 20% decrease in extracellular fosamine by Fe-deficient *P. megaterium* suggested a possible contribution of fosamine to carbon influx that needs to be confirmed (Appendix C, SI). In sum, our data revealed that the suppressed specific growth rates (relative to control) in Fe-deficient cells of both species exposed to phosphonate herbicides did not result from the inhibition of the substrate uptake. To gain insights on metabolic disruptions by each phosphonate herbicide, we performed a metabolomics analysis of the metabolic pathways involved in the biosynthesis of various plant-beneficial compounds such as auxins, siderophores, and antibiotics.

Phosphonate Herbicides Induce Auxin Production in Fe-Replete Cells

We monitored the levels of the following metabolites associated with pathways associated with auxin biosynthesis in each species: S3P, a precursor to aromatic amino acids and auxins; two aromatic amino acids (phenylalanine and

tyrosine); and two auxins (phenylacetic acid and indole-3-acetic acid) (Figure 3A). In Fe-replete glyphosate-exposed cells, a 79% increase in S3P in *P. protegens* cells at 1 mM glyphosate dose ($p = 0.024$) (Figure 3B; Appendix D, SI) and a 50-fold increase in S3P in *P. megaterium* cells ($p \leq 0.003$) (Figure 3C; Appendix E, SI) were consistent with the inhibition of EPSP synthase as the target of glyphosate as previously reported.⁴² The lack of accumulation of S3P in both glufosinate-exposed or fosamine-exposed Fe-replete *P. protegens* cells implied that EPSP synthase may not be targeted by the two herbicides in *P. protegens* (Figure 3B; Appendix D, SI). In contrast, we obtained a 2.5-fold increase in S3P ($p = 0.013$) at 0.1 mM glufosinate dose and up to a 4.6-fold increase in S3P ($p \leq 0.046$) across all fosamine doses in Fe-replete *P. megaterium* cells (Figure 3C; Appendix E, SI), suggesting that both glufosinate and fosamine also had an inhibitory effect on EPSP synthase in *P. megaterium*.

Despite the inhibition of EPSP synthase (as indicated by the accumulation of S3P) in response to glyphosate exposure, there was no change in the intracellular levels of either phenylalanine or tyrosine in Fe-replete *P. protegens* cells ($p \geq 0.135$), implying that the biosynthetic flux toward the aromatic amino acids was not impaired (Figure 3B; Appendix D, SI). For Fe-replete *P. megaterium* cells, while a 1 mM glyphosate dose led to a 37% increase in phenylalanine ($p = 0.019$) and no statistically significant change in tyrosine ($p = 0.102$) in Fe-replete *P. megaterium* cells, the level of phenylalanine and tyrosine at 0.5 mM glyphosate dose was decreased by 90% ($p = 0.006$) and 45% ($p = 0.038$), respectively (Figure 3C; Appendix E, SI). Therefore, the adverse effect of glyphosate on aromatic amino acid biosynthesis was dose-dependent in Fe-replete *P. megaterium* cells.

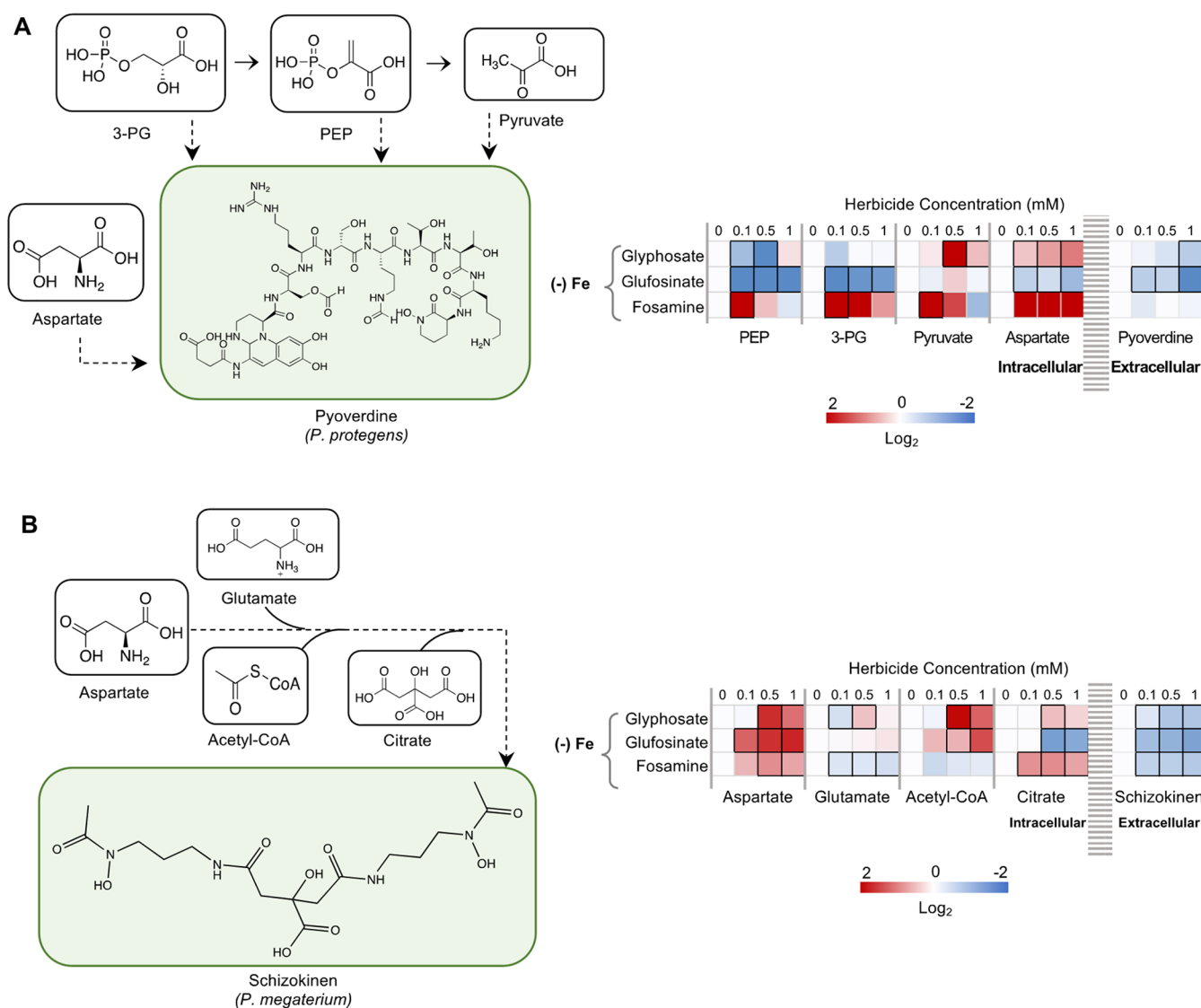


Figure 4. Effects of herbicide exposure on levels of metabolite precursors and secretions of (A) siderophore pyoverdine by *P. protegens* and (B) schizokinen by *P. megaterium* cells grown under Fe-limited [(-)Fe] conditions. All data are shown relative to control experiment without any herbicide in the nutrient medium. In the heat maps, statistically significant differences, which were calculated from unpaired two-tailed *t* test analyses, $p < 0.05$, are indicated by a black border. Metabolite abbreviations: PEP, phosphoenolpyruvate; 3-PG, 3-phosphoglycerate; acetyl-CoA, acetyl coenzyme A.

During the exposure to glufosinate, the phenylalanine pool remained unchanged in Fe-replete *P. megaterium* cells ($p \geq 0.063$), whereas the tyrosine level was decreased by 21–25% in Fe-replete *P. megaterium* cells at 0.1 and 1 mM glufosinate doses ($p \leq 0.028$) (Figure 3C; Appendix E, SI). For fosamine-exposed Fe-replete cells, there was up to an 11-fold increase in phenylalanine in *P. megaterium* across all fosamine doses ($p \leq 0.001$) but a 32–43% depletion in tyrosine at 0.1–0.5 mM fosamine doses ($p \leq 0.013$) (Figure 3C, Appendix E, SI). These data indicated that glufosinate and fosamine might not target the biosynthesis of phenylalanine but may interfere with tyrosine biosynthesis in Fe-replete *P. megaterium* cells.

We evaluated the effects of the aforementioned changes in the shikimate pathway and aromatic amino acid biosynthesis on auxin production in both *P. protegens* and *P. megaterium* (Figure 3A). Under the Fe-replete conditions, there was a 39–69% increase in secreted phenylacetic acid in *P. protegens* at 0.1–1 mM glyphosate doses ($p \leq 0.008$) (Figure 3B; Appendix D, SI), and there was a 3.7-fold increase in secreted

indole-3-acetic acid in *P. megaterium* cells exposed at 1 mM glyphosate dose ($p < 0.001$) (Figure 3C; Appendix E, SI). For Fe-replete glufosinate-exposed cells, the auxin level was increased by 39% in *P. protegens* cells at 0.1 mM glufosinate dose ($p = 0.016$) (Figure 3B; Appendix D, SI) and 42–79% in *P. megaterium* cells at 0.5–1 mM glufosinate doses ($p \leq 0.023$) (Figure 3C; Appendix E, SI). Similarly, there was a 24–40% increase in secreted phenylacetic acid at 0.5–1 mM fosamine doses in *P. protegens* cells ($p \leq 0.018$) (Figure 3B; Appendix D, SI) and a 27% increase in indole-3-acetic acid secretion in *P. megaterium* cells at 0.5 mM fosamine dose ($p = 0.043$) (Figure 3C; Appendix E, SI). Therefore, for both species, our data revealed that exposure to the phosphonate herbicides promoted auxin secretion under Fe-replete nutrient conditions, regardless of apparent metabolic disruption in the shikimate pathway.

Inhibition of Auxin Secretion by Phosphonate Herbicides in Fe-Deficient Cells

In contrast to the increased auxin secretion in Fe-replete cells, both Fe-deficient *P. protegens* and *P. megaterium* cells exhibited a decrease in auxin secretion during exposure to phosphonate herbicides relative to control (Figure 3B,C). Specifically, for the glyphosate-exposed Fe-deficient cells, the level of secreted phenylacetic acid in *P. protegens* cells was decreased by up to 83% ($p \leq 0.025$) (Figure 3B; Appendix D, SI), and there was up to a 2-fold depletion in indole-3-acetic acid in *P. megaterium* cells ($p \leq 0.008$) (Figure 3C, Appendix E, SI). Interestingly, there were no changes in levels of both S3P ($p = 0.168$) and phenylalanine ($p \geq 0.308$) in Fe-deficient *P. protegens* cells at 1 mM glyphosate dose (Figure 3B; Appendix D, SI). However, there was at least a 50-fold accumulation of S3P ($p \leq 0.001$) and up to a 10-fold depletion in phenylalanine ($p \leq 0.001$) in Fe-deficient *P. megaterium* cells in response to the glyphosate doses ($p \leq 0.001$) (Figure 3C; Appendix E, SI), highlighting again the inhibition of ESPS synthase as the specific toxic action of glyphosate in *P. megaterium*.

During the exposure to glufosinate, the secreted auxin level was decreased by up to 79% in Fe-deficient *P. protegens* cells ($p \leq 0.009$) (Figure 3B, Appendix D, SI) and 76% in Fe-deficient *P. megaterium* cells ($p \leq 0.003$) (Figure 3C, Appendix E, SI). Similarly, the exposure of fosamine led to up to a 23-fold depletion in secreted phenylacetic acid in Fe-deficient *P. protegens* cells ($p \leq 0.001$) (Figure 3B; Appendix D, SI) and a 32% decrease in indole-3-acetic acid in Fe-deficient *P. megaterium* cells at 1 mM fosamine dose ($p < 0.001$) (Figure 3C, Appendix E, SI). The phenylalanine level was also depleted in response to glufosinate exposure in Fe-deficient cells of both species (Figure 3B,C). Specifically, there were up to 2.7-fold and 2-fold depletions in the phenylalanine level in Fe-deficient *P. protegens* cells ($p \leq 0.001$) and *P. megaterium* cells ($p \leq 0.003$), respectively (Figure 3B,C; Appendices D and E, SI). Across the exposure to the different phosphonate herbicides at the various doses, the tyrosine pool was reduced by up to 59% in Fe-deficient *P. megaterium* cells ($p \leq 0.049$) but was increased (by up to 6-fold) in Fe-deficient *P. protegens* cells ($p \leq 0.042$) (Figure 3B,C; Appendices D and E, SI). With respect to the S3P level during glufosinate or fosamine exposure, it was unchanged or decreased by at least 18% in Fe-deficient *P. megaterium* cells ($p \leq 0.016$) (Figure 3C; Appendix E, SI), and there was up to 93% decrease in S3P in Fe-deficient *P. protegens* cells ($p \leq 0.060$) (Figure 3B; Appendix E, SI), indicating the lack of inhibitory effect on EPSP synthase in the presence of glufosinate and fosamine but a decrease in carbon flux through the shikimate pathways toward antibiotic secretion. In sum, our data indicated that exposure to the phosphonate herbicides consistently resulted in the depletion of auxin production in both Fe-deficient *P. protegens* and *P. megaterium* cells, which was accompanied by either decreased carbon flux upstream of the shikimate pathway or inhibition of the EPSP synthase within the shikimate pathway.

Siderophore Production Is Impaired in Fe-Deficient Herbicide-Exposed Cells

First, we considered the precursor metabolites to the biosynthesis of pyoverdine siderophores in Fe-deficient *P. protegens* and schizokinen biosynthesis in Fe-deficient *P. megaterium* (Figure 4). Specifically, we evaluated the intracellular levels of PEP, 3-PG, pyruvate, and aspartate in the biosynthetic pathway of pyoverdine in *P. protegens* Pf-5 (Figure

4A); we evaluated the intracellular levels of aspartate, glutamate, acetyl-CoA, and citrate in the biosynthetic pathway of schizokinen in *P. megaterium* (Figure 4B). Relative to control, fosamine exposure did not result in any decline in the precursors (including PEP, 3-PG, pyruvate, and aspartate) to pyoverdine biosynthesis ($p \geq 0.054$), which was consistent with no change in secreted pyoverdine in fosamine-exposed Fe-deficient *P. protegens* cells ($p \geq 0.236$) (Figure 4A; Appendix F, SI). In comparison, although fosamine exposure caused no change in acetyl-CoA ($p \geq 0.143$), a 62–85% increase in aspartate ($p \leq 0.018$), and a near 3-fold increase in citrate ($p \leq 0.016$), the glutamate level was decreased by 23–30% ($p \leq 0.027$) in Fe-deficient *P. megaterium* cells, all of which was consistent with the 40–46% depletion in secreted schizokinen in Fe-deficient fosamine-exposed *P. megaterium* cells ($p \leq 0.002$) (Figure 4B; Appendix G, SI). In the presence of glyphosate, Fe-deficient *P. protegens* cells exhibited up to a 92% depletion in PEP at 0.1–0.5 mM glyphosate doses ($p \leq 0.002$), up to a 4.5-fold increase in pyruvate at 0.5–1 mM glyphosate doses ($p \leq 0.004$), up to a 2-fold increase in aspartate during glyphosate exposure ($p \leq 0.017$) and a near 2-fold depletion in pyoverdine at 1 mM dose ($p = 0.027$) (Figure 4A; Appendix F, SI). Moreover, a 0.1 mM glyphosate dose caused a 29% decrease in glutamate in Fe-deficient *P. megaterium* cells ($p < 0.001$), but there was about a 40% increase in both glutamate ($p = 0.007$) and citrate ($p = 0.045$) levels at 0.5 mM glyphosate dose, and up to a 3-fold and 4-fold increase, respectively, in aspartate ($p \leq 0.001$) and acetyl-CoA ($p \leq 0.004$) at 0.5–1 mM glyphosate doses (Figure 4B; Appendix G, SI). Along with this accumulation in three of the four precursor metabolites to the biosynthesis of the siderophore schizokinen in Fe-deficient glyphosate-exposed *P. megaterium* cells, we found that the secreted amount of schizokinen was reduced by up to 48% ($p \leq 0.012$) (Figure 4B; Appendix G, SI). Glufosinate exposure led to a 76–86% depletion in PEP ($p \leq 0.001$), a 70–80% decrease in 3-PG ($p \leq 0.016$), a 31–55% reduction in aspartate ($p \leq 0.008$), and up to a 4.3-fold depletion in pyoverdine in Fe-deficient *P. protegens* cells ($p \leq 0.038$) (Figure 4A; Appendix F, SI). In Fe-deficient glufosinate-exposed *P. megaterium* cells, besides up to a 3-fold increase in aspartate ($p \leq 0.038$) and acetyl-CoA ($p \leq 0.030$), there was a 63–38% decrease in citrate ($p \leq 0.008$) and greater than 70% reduction in secreted schizokinen ($p \leq 0.001$) (Figure 4B; Appendix G, SI). Therefore, our data revealed that phosphonate herbicides impaired siderophore production in the Fe-deficient cells of both species except for no change in fosamine-exposed Fe-deficient *P. protegens* cells (Figure 4). Furthermore, we found that glufosinate had the greatest adverse effects on siderophore production in both species (Figure 4).

Phosphonate Herbicides Induce Antibiotic Secretion in Fe-Replete *P. protegens* Cells

To gain insights into the biosynthesis and subsequent secretion of antibiotics in *P. protegens* Pf-5 cells exposed to phosphonate herbicides, we profiled metabolites associated with the biosynthetic pathway of DAPG and pyoluteorin (Figure 5). In relation to DAPG biosynthesis, we evaluated the following metabolites: acetyl-CoA and phloroglucinol, two precursors to DAPG secretion; and PG-Cl, a regulator of DAPG biosynthesis derived from phloroglucinol to induce pyoluteorin production⁴⁸ (Figure 5A). With respect to precursors to pyoluteorin biosynthesis, we measured α -KG and glutamate (Figure 5B).

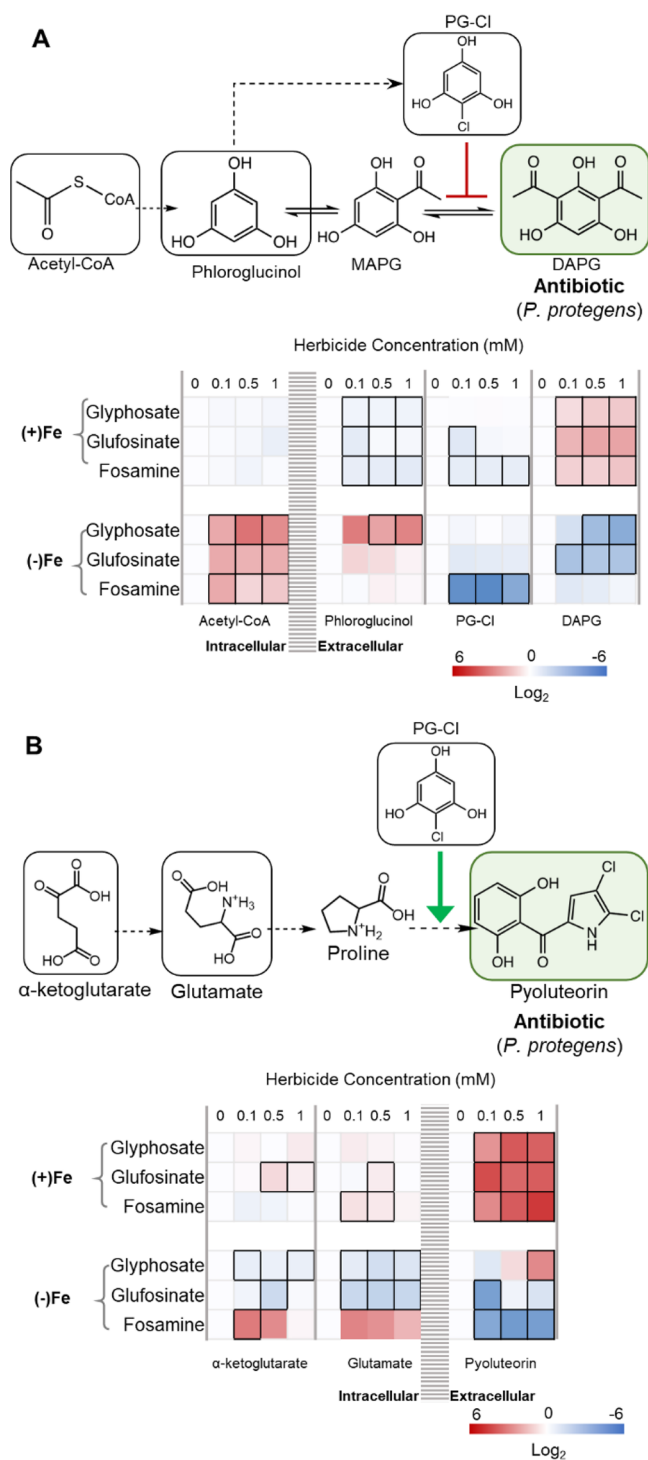


Figure 5. Effects of herbicide exposure on the production of the antibiotics (A) DAPG and (B) pyoluteorin by *P. protegens* cells grown under (top) Fe-replete [(+)Fe] and (bottom) Fe-limited [(-)Fe] conditions. All data are shown relative to control (in the absence of any herbicide) in the respective nutrient condition. In the reaction scheme, the measured metabolites are boxed: metabolite precursors and a metabolic regulator (white); antibiotic compounds (green). Solid and dashed arrows refer to the occurrence of one reaction versus multiple reactions, respectively, between two metabolites. In the heat maps, statistically significant differences, which were calculated from unpaired two-tailed *t* test analyses, $p < 0.05$, are indicated by a black border. Metabolite abbreviations: MAPG, monoacetyl-phloroglucinol; PG-Cl, 2-chlorobenzene-1,3,5-triol; DAPG, 2,4-diacetylphloroglucinol.

In Fe-replete *P. protegens* Pf-5 cells exposed to phosphonate herbicides, no statistically significant change in acetyl-CoA ($p \geq 0.193$) and a 16–47% reduction in phloroglucinol ($p \leq 0.031$) were accompanied by an increase in the secreted DAPG (Figure 5A; Appendix H, SI). Specifically, DAPG secretion was increased by up to 2.3-fold ($p \leq 0.030$), 2.5-fold ($p \leq 0.001$), and 4.3-fold ($p \leq 0.017$), respectively, in the presence of glyphosate, fosamine, and glufosinate in Fe-replete *P. protegens* cells (Figure 5A; Appendix H, SI). There was no change in the level of the regulating compound, PG-Cl, when Fe-replete *P. protegens* cells were exposed to glyphosate ($p \geq 0.269$), whereas the PG-Cl level was decreased by 51% at 0.1 mM glufosinate dose ($p = 0.001$) and about 42% at the varying fosamine doses ($p \leq 0.005$) (Figure 5A; Appendix H, SI). Thus, our data revealed that phosphonate herbicides induced the antibiotic DAPG secretion in Fe-replete *P. protegens* cells.

Regarding the pyoluteorin biosynthesis in Fe-replete *P. protegens* cells, glyphosate exposure led to no statistically significant change in the precursor α -KG and glutamate ($p \geq 0.052$) (Figure 5B; Appendix I, SI). For Fe-replete fosamine-exposed *P. protegens* cells, the α -KG level was still not statistically significantly changed ($p \geq 0.085$), but the glutamate level was increased by 39–58% at 0.1–0.5 mM fosamine doses ($p \leq 0.005$) (Figure 5B; Appendix I, SI). At 0.5 mM glufosinate doses, Fe-replete *P. protegens* cells exhibited an 80% elevation in α -KG ($p = 0.004$) and a 34% increase in glutamate ($p = 0.032$) (Figure 5B; Appendix I, SI). The accumulation in glutamate in the presence of glufosinate was consistent with the inhibition of glutamine synthetase, in accordance with the aforementioned mode of toxic action of glufosinate. In Fe-replete *P. protegens* cells, we obtained up to a 15-fold increase in secreted pyoluteorin in the presence of glyphosate ($p \leq 0.001$), up to an 18-fold increase at the varying doses of glufosinate ($p \leq 0.001$), and up to a 25-fold increase in the presence of fosamine ($p \leq 0.006$) (Figure 5B; Appendix I, SI). In sum, under Fe-replete conditions, our data emphasized the role of phosphonate herbicides in increasing the secretion of both antibiotics, DAPG and pyoluteorin, produced by *P. protegens* cells.

Iron Deficiency Inhibits Antibiotic Secretion in Herbicide-Exposed Cells

In Fe-deficient *P. protegens* cells exposed to phosphonate herbicides except for the 0.1 mM glufosinate dose, the acetyl-CoA level was increased by up to 10-fold ($p \leq 0.006$), indicating a triggered metabolic bottleneck (Figure 5A; Appendix H, SI). The extracellular phloroglucinol level was also elevated by up to 7-fold at 0.5–1 mM glyphosate doses ($p \leq 0.007$) (Figure 5A; Appendix H, SI). Exposure to glufosinate or fosamine did not result in any statistically significant change in phloroglucinol level in Fe-deficient *P. protegens* cells ($p \geq 0.130$) (Figure 5A; Appendix H, SI). In contrast to no less than a 68% increase in DAPG secretion in the Fe-replete ($p \leq 0.030$), DAPG secretion was decreased in Fe-deficient cells exposed to two of the phosphonate herbicides (Figure 5A; Appendix H, SI). Specifically, for Fe-deficient glufosinate-exposed *P. protegens* cells, DAPG secretion was decreased by about 86% ($p \leq 0.046$) and there was an 18-fold depletion in DAPG in Fe-deficient *P. protegens* cells at 1 mM glyphosate dose ($p = 0.036$) (Figure 5A; Appendix H, SI). There was no change in the DAPG secretion in response to fosamine exposure ($p \geq 0.195$) (Figure 5A; Appendix H, SI). These data imply that iron deficiency compromised DAPG secretion

during the exposure to glyphosate and glufosinate and the biosynthesis of DAPG was more susceptible to glufosinate than glyphosate and fosamine in Fe-deficient *P. protegens* cells. Moreover, the regulating compound PG-Cl was completely depleted in the presence of fosamine ($p \leq 0.005$), but there was no change in PG-Cl level with glyphosate or glufosinate ($p \geq 0.077$) (Figure 5A; Appendix H, SI).

Regarding the pyoluteorin biosynthesis in Fe-deficient *P. protegens* cells, there was an 8.5-fold increase in α -KG at 0.1 mM fosamine dose ($p = 0.002$), a 39% depletion at 0.1 mM glyphosate dose ($p = 0.030$), and a 62% decrease at 0.5 mM glufosinate dose ($p = 0.002$) (Figure 5B; Appendix I, SI). Relative to control, there was no change in glutamate in Fe-deficient fosamine-exposed cells ($p \geq 0.062$), but the glutamate level was reduced by up to 65% in the presence of glyphosate ($p \leq 0.001$) and by ~75% in response to glufosinate doses ($p \leq 0.001$) (Figure 5B; Appendix I, SI). The secreted pyoluteorin was increased by 6.7-fold at 1 mM glyphosate dose ($p = 0.005$) (Figure 5B; Appendix I, SI). With glufosinate, the Fe-deficient *P. protegens* cells exhibited a 96% ($p = 0.001$) and 59% ($p = 0.013$) depletion in secreted pyoluteorin, respectively, at 0.1 and 1 mM glufosinate doses (Figure 5B; Appendix I, SI). For Fe-deficient fosamine-exposed *P. protegens* cells, there was no less than a 21-fold depletion in pyoluteorin secretion ($p \leq 0.001$) (Figure 5B; Appendix I, SI). Collectively, our data revealed that iron deficiency exerted adverse effects on the biosynthesis of antibiotic secretion in herbicide-exposed *P. protegens* cells.

DISCUSSION

Here we sought to shed light on how exposure to three widely used phosphonate herbicides may affect biomass growth rates, cellular metabolism, and secretions of plant-beneficial compounds in two relevant PGPR species: *P. protegens* (a Gram-negative bacterium) and *P. megaterium* (a Gram-positive bacterium). Overall, we found that the growth of *P. megaterium* cells was more susceptible to the phosphonate herbicides than the *P. protegens* cells (Figure 1B,C). Consistent with our growth phenotype data, it was reported previously⁶⁰ that the application of herbicides led to a decrease in the relative abundance of Gram-positive bacteria, whereas there was no statistically significant change in the relative abundance of Gram-negative bacteria. The composition of the fatty acids in the cytoplasmic membrane of Gram-negative aerobic bacteria has been implicated in facilitating the tolerance of these bacteria to high concentration of contaminants, including herbicides.⁶¹ In the introduction, we had put forth three hypotheses regarding the effects of phosphonate herbicides on the production of plant-beneficial compounds produced by the two investigated PGPR.

Regarding the first hypothesis, our data revealed a decrease in auxin production in the Fe-deficient *P. protegens* and *P. megaterium* cells grown in the presence of phosphonate herbicides, but there was an enhanced production of auxins in the Fe-replete cells of both species exposed to herbicides (Figure 3). With respect to the disruption of the shikimate pathway associated with the change in auxin production, we obtained accumulation of S3P in Fe-replete glyphosate-exposed cells of both *P. protegens* and *P. megaterium* (Figure 3), indicating that glyphosate targeted EPSP synthase in both PGPR bacteria similarly to plants. Despite determining only about 25–30% similarity in EPSP synthase sequence between plants (*Arabidopsis thaliana*) and PGPR species (*P. protegens*

and *P. megaterium*) (Appendix J, SI), the binding site for both glyphosate and the endogenous substrate PEP was reported to be highly conserved in the in EPSP synthases of the plants and PGPR species^{62,63} thus explaining the similar toxic effect of glyphosate.

Glyphosate was reported to inhibit auxin secretion in *Klebsiella sp.* strain PS19,⁶⁴ but the relationship between metabolism and effects of glyphosate and other phosphonate herbicides on auxin secretion in PGPR were not yet investigated. Interestingly, in Fe-replete glyphosate-exposed *P. protegens* cells, the observed inhibition of EPSP synthase (as evidenced by the accumulation of S3P) did not result in a decline in the secretion of the auxin phenylacetic acid, which was instead enhanced (Figure 3B). However, with the Fe-deficient *P. protegens* cells, exposure to glyphosate resulted in depletion or no change of S3P, accompanied by decreased secretion of phenylacetic acid. These findings indicated that the metabolic flux for auxin biosynthesis was sustained in Fe-replete cells but was impaired in Fe-depleted cells. Similar to the *P. protegens* cells, the *P. megaterium* cells exposed to all three herbicide exposures resulted in the promoted secretion of the specific auxin (indole-3-acetic acid) under the Fe-replete conditions but decreased secretion under the Fe-limited condition. Beyond glyphosate-induced accumulation of S3P in both Fe-replete and Fe-deficient *P. megaterium*, we found that exposure to the other two herbicides also resulted in elevated levels of S3P in the Fe-replete cells, suggesting potential EPSP synthase inhibition by these herbicides in *P. megaterium*. The gene *yhhS*, which encodes a membrane efflux transporter in *Escherichia coli* was reported to serve as a potential glyphosate resistance mechanism.⁶⁵ Given the occurrence of the *yhhS* gene also in *Pseudomonas* species,⁶² it remains to be investigated whether the higher tolerance of *P. protegens* than *P. megaterium* to glyphosate and other herbicide exposures may be due to herbicide export outside of cells by membrane efflux transporters.

With respect to the second hypothesis, we consistently obtained a decrease in siderophore production by the Fe-deficient *P. protegens* and *P. megaterium* exposed to the different phosphonate herbicides, as well as the observations of metabolic perturbations in central carbon metabolism that were consistent with decreased siderophore biosynthesis (Figure 4). Specifically, we obtained a decrease in the cellular levels of different metabolite precursors (PEP, 3-PG, or aspartate) to the biosynthesis of the siderophore pyoverdine in Fe-deficient *P. protegens* cells (Figure 4A) and metabolite precursors (citrate or glutamate) to the biosynthesis of the siderophore schizokinen in Fe-deficient *P. megaterium* cells (Figure 4B). A previous study reported that glyphosate suppressed the siderophore secretion in several plant growth-promoting rhizobacteria,⁶⁶ but the effects of other phosphonate herbicides (i.e., glufosinate and fosamine) on siderophore secretion by soil bacteria were not evaluated. Here, in addition to glyphosate, our results showed that both glufosinate and fosamine exposures led to impaired siderophore biosynthesis (Figure 4).

Regarding the third hypothesis, decreased secretion of the antibiotics DAPG and pyoluteorin was only obtained with Fe-deficient herbicide-exposed *P. protegens* cells whereas there was substantial increase in the antibiotic secretion in Fe-replete *P. protegens* cells (Figures 5). With respect to the specific effects of glufosinate on the antibiotic biosynthetic pathway, we did obtain accumulation in glutamate in Fe-replete *P. protegens*

cells at 0.5 mM glufosinate dose and an associated increase in pyoluteorin secretion, suggesting that the flux to pyoluteorin production was facilitated by the increase in the precursor glutamate due to inhibition of glutamine synthetase despite only about a 22% identity similarity between the sequences of glutamine synthetase in plants (*Triticum aestivum*) and *P. protegens* Pf-5 (Appendix K, SI). A previous study proposed that the gene cluster *pltIJKNOP* involved in the biosynthesis of pyoluteorin in *P. protegens* Pf-5 cells may also be responsible for encoding pyoluteorin transporters.⁶⁷ For instance, the transcripts of the pyoluteorin efflux transporter genes, *pltI* and *pltJ*, were enhanced by increased exogenous pyoluteorin,⁶⁷ consistent with a reported positive autoregulation of pyoluteorin secretion.⁶⁸ Thus, in addition to our observed increase in the metabolite precursors, the accumulation of pyoluteorin in glufosinate-exposed Fe-replete *P. protegens* cells might be a result of the positive autoregulation of pyoluteorin. By contrast, there was a depletion in glutamate accompanied by a decrease in secreted pyoluteorin in glufosinate-exposed Fe-deficient *P. protegens* cells (Figure 5B). The antibiotic DAPG was also reported to autoinduce the expression of the operon, *phlACBD*, which is involved in the biosynthesis of DAPG in *P. fluorescens* CHA0⁶⁹ and *P. fluorescens* 2P24.⁷⁰ Thus, it remains to be investigated whether the increased DAPG secretion in Fe-replete herbicide-exposed *P. protegens* cells was due to a similar regulation. Furthermore, in Fe-limited *P. protegens*, the genes involved in the biosynthesis of DAPG are known to encode a transcriptional repressor PhIF that down-regulates the biosynthesis of DAPG.⁷¹ Therefore, further investigation is needed to determine to what extent the measured decrease in DAPG secretion in herbicide-exposed Fe-deficient *P. protegens* was a consequence of the metabolic changes induced by the herbicide exposure versus the suppression of DAPG biosynthesis under Fe limitation.

In sum, the findings in the present study highlighted an increase in secreted plant-beneficial compounds by the investigated PGPR species in nutrient replete conditions but compromised cellular metabolism in nutrient deficient conditions which facilitated the adverse effects of the phosphonate herbicides on the production of beneficial compounds. Because the data were obtained with experiments conducted with soil-free media, our findings provided insights on direct exposure of PGPR to the phosphonate herbicides within the soil solution. We acknowledge the potential adsorption of glyphosate,^{72–78} glufosinate,^{79,80} and fosamine⁸¹ onto soil mineral particles, thereby potentially modulating the exposure of phosphonate herbicides to PGPR. Studies on the mobility and the subsequent bioavailability of adsorbed herbicides are needed to evaluate the relevance of our findings in relation to the bioavailability of accumulated phosphonate herbicide residues in agricultural soils. Microcosm experiments with natural soils would be helpful to shed light on the effects of herbicide exposure on bacteria and crops under natural soil conditions. In addition to the active herbicide ingredients, it is important to point out that herbicide formulations contain additives including surfactants, which have been shown to exert adverse metabolic outcomes in beneficial soil *Pseudomonas* species.⁵³ However, it is not yet known the extent to which these metabolic effects of formulation additives may impact the microbial production of plant-beneficial compounds. Here our study has focused on investigating species from two different genera of PGPR with important relevance to current biocontrol applications. Subsequent investigations on the

metabolic effects of phosphonate herbicide exposures on other PGPR genera will be instrumental toward gaining further insights on the potential effects of these herbicides on the soil microbiome.

■ ASSOCIATED CONTENT

SI Supporting Information

The Supporting Information is available free of charge at <https://pubs.acs.org/doi/10.1021/acsenvironau.1c00030>.

Supporting figures and tables referred to in the main text as Appendices A–K (PDF)

■ AUTHOR INFORMATION

Corresponding Author

Ludmilla Aristilde – Department of Chemical and Biological Engineering, McCormick School of Engineering and Applied Science, Northwestern University, Evanston, Illinois 60208, United States; Department of Biological and Environmental Engineering, College of Agriculture and Life Sciences, Cornell University, Ithaca, New York 14853, United States; Department of Civil and Environmental Engineering, McCormick School of Engineering and Applied Science, Northwestern University, Evanston, Illinois 60208, United States; orcid.org/0000-0002-8566-1486; Email: ludmilla.aristilde@northwestern.edu

Authors

Wenting Li – Department of Chemical and Biological Engineering, McCormick School of Engineering and Applied Science, Northwestern University, Evanston, Illinois 60208, United States

Rebecca A. Wilkes – Department of Biological and Environmental Engineering, College of Agriculture and Life Sciences, Cornell University, Ithaca, New York 14853, United States; Department of Civil and Environmental Engineering, McCormick School of Engineering and Applied Science, Northwestern University, Evanston, Illinois 60208, United States

Complete contact information is available at:

<https://pubs.acs.org/10.1021/acsenvironau.1c00030>

Author Contributions

W.L. and L.A. designed the research and drafted the manuscript. W.L. and R.A.W. conducted the research. W.L. and L.A. analyzed the data. L.A. supervised the research. All authors provided critical revisions to the manuscript.

Notes

The authors declare no competing financial interest.

■ ACKNOWLEDGMENTS

This research was funded by a CAREER research grant awarded to L.A. from the U.S. National Science Foundation (CBET-1653092). We are grateful to Dr Bahareh Hassanpour of the Aristilde Research Group for her technical assistance during the LC-MS analyses. We thank Dr Keith E. J. Tyo (Department of Chemical and Biological Engineering) and Dr Erica Hartmann (Department of Civil and Environmental Engineering) for their insightful critical comments on early manuscript drafts.

REFERENCES

- (1) Benbrook, C. M. Trends in glyphosate herbicide use in the United States and globally. *Environ. Sci. Eur.* **2016**, *28* (1), 3.
- (2) Takano, H. K.; Dayan, F. E. Glufosinate-ammonium: a review of the current state of knowledge. *Pest Manage. Sci.* **2020**, *76* (12), 3911–3925.
- (3) Annett, R.; Habibi, H. R.; Hontela, A. Impact of glyphosate and glyphosate-based herbicides on the freshwater environment. *J. Appl. Toxicol.* **2014**, *34* (5), 458–479.
- (4) United States Geological Survey (USGS). *Estimated Agricultural Use for Glufosinate, 2017. Pesticide National Synthesis Project*. https://water.usgs.gov/nawqa/pnsp/usage/maps/show_map.php?year=2017&map=GLUFOSINATE&hilo=L (accessed 15 October 2021).
- (5) Washington State Department of Transportation. *Fosamine Roadside Vegetation Management Herbicide Fact Sheet*. <https://wsdot.wa.gov/sites/default/files/2021-10/Herbicides-factsheet-Fosamine.pdf> (accessed November 17, 2021 at URL).
- (6) Horsman, G. P.; Zechel, D. L. Phosphonate Biochemistry. *Chem. Rev.* **2017**, *117* (8), 5704–5783.
- (7) Hanke, I.; Wittmer, I.; Bischofberger, S.; Stamm, C.; Singer, H. Relevance of urban glyphosate use for surface water quality. *Chemosphere* **2010**, *81* (3), 422–429.
- (8) Kanissery, R.; Gairhe, B.; Kadyampakeni, D.; Batuman, O.; Alferes, F. Glyphosate: Its Environmental Persistence and Impact on Crop Health and Nutrition. *Plants* **2019**, *8* (11), 499.
- (9) Jaiswal, D. K.; Verma, J. P.; Yadav, J.; Singh, S. Microbe Induced Degradation of Pesticides in Agricultural Soils. *Environ. Sci. Eng.* **2017**, *167*.
- (10) Hussain, T.; Akthar, N.; Aminedi, R.; Danish, M.; Nishat, Y.; Patel, S.; Singh, J.; Yadav, A. Role of the Potent Microbial Based Bioagents and Their Emerging Strategies for the Ecofriendly Management of Agricultural Phytopathogens. *Nat. Bioactive Prod. Sustain. Agric.* **2020**, 45.
- (11) Tripathi, A. N.; Meena, B. R.; Pandey, K. K.; Singh, J.; Rakshit, A.; Singh, H.; Singh, A.; Singh, U.; Fraceto, L. Microbial Bioagents in Agriculture: Current Status and Prospects. *New Frontiers in Stress Management for Durable Agriculture*. **2020**, 331.
- (12) Kloepper, J. W.; Schroth, M. N. Plant growth promoting rhizobacteria and plant growth under gnotobiotic conditions. *Phytopathology* **1981**, *71*, 642–644.
- (13) Davison, J. Plant Beneficial Bacteria. *Nat. Biotechnol.* **1988**, *6*, 282–286.
- (14) Imfeld, G.; Vuilleumier, S. Measuring the effects of pesticides on bacterial communities in soil: A critical review. *Eur. J. Soil Biol.* **2012**, *49*, 22–30.
- (15) Ramette, A.; Frapolli, M.; Fischer-Le Saux, M.; Gruffaz, C.; Meyer, J. M.; Défago, G.; Sutra, L.; Moënne-Loccoz, Y. *Pseudomonas protegens* sp. nov., widespread plant-protecting bacteria producing the biocontrol compounds 2,4-diacetylphloroglucinol and pyoluteorin. *Syst. Appl. Microbiol.* **2011**, *34* (3), 180–188.
- (16) Gupta, R. S.; Patel, S.; Saini, N.; Chen, S. Robust demarcation of 17 distinct *Bacillus* species clades, proposed as novel Bacillaceae genera, by phylogenomics and comparative genomic analyses: description of *Robertmurraya kyonggiensis* sp. nov. and proposal for an emended genus *Bacillus* limiting it only to the members of the *Subtilis* and *Cereus* clades of species. *Int. J. Syst. Evol. Microbiol.* **2020**, *70* (11), 5753–5798.
- (17) Setten, L.; Soto, G.; Mozzicafreddo, M.; Fox, A. R.; Lisi, C.; Cuccioloni, M.; Angeletti, M.; Pagano, E.; Diaz-Paleo, A.; Ayub, N. D. Engineering *Pseudomonas protegens* Pf-5 for nitrogen fixation and its application to improve plant growth under nitrogen-deficient conditions. *PLoS One* **2013**, *8* (5), e63666.
- (18) Xie, Y.; Liu, Z.; Zhang, G.; Mo, X.; Ding, X.; Xia, L.; Hu, S. A rifampicin-resistant (rpoB) mutation in *Pseudomonas protegens* Pf-5 strain leads to improved antifungal activity and elevated production of secondary metabolites. *Res. Microbiol.* **2016**, *167* (8), 625–629.
- (19) Nascimento, F. X.; Hernández, A. G.; Glick, B. R.; Rossi, M. J. Plant growth-promoting activities and genomic analysis of the stress-resistant *Bacillus megaterium* STB1, a bacterium of agricultural and biotechnological interest. *Biotechnol. Rep. (Amst)* **2020**, *25*, e00406.
- (20) Trivedi, P.; Pandey, A. Plant growth promotion abilities and formulation of *Bacillus megaterium* strain B 388 (MTCC6521) isolated from a temperate Himalayan location. *Indian J. Microbiol.* **2008**, *48* (3), 342–347.
- (21) Radhakrishnan, R.; Hashem, A.; Abd Allah, E. F.; et al. *Bacillus*: A Biological Tool for Crop Improvement through Bio-Molecular Changes in Adverse Environments. *Front. Physiol.* **2017**, *8*, 667.
- (22) Loper, J. E.; Hassan, K. A.; Mavrodi, D. V.; Davis, E. W.; Lim, C. K.; Shaffer, B. T.; Elbourne, L. D. H.; Stockwell, V. O.; Hartney, S. L.; Breakwell, K.; Henkels, M. D.; Tetu, S. G.; Rangel, L. I.; Kidarsa, T. A.; Wilson, N. L.; van de Mortel, J. E.; Song, C.; Blumhagen, R.; Radune, D.; Hostetler, J. B.; Brinkac, L. M.; Durkin, A. S.; Kluepfel, D. A.; Wechter, W. P.; Anderson, A. J.; Kim, Y. C.; Pierson, L. S.; Pierson, E. A.; Lindow, S. E.; Kobayashi, D. Y.; Raaijmakers, J. M.; Weller, D. M.; Thomashow, L. S.; Allen, A. E.; Paulsen, I. T. Comparative Genomics of Plant-Associated *Pseudomonas* spp.: Insights into Diversity and Inheritance of Traits Involved in Multitrophic Interactions. *PLoS Genet.* **2012**, *8* (7), e1002784.
- (23) Lee, J. C.; Whang, K. S. Optimization of Indole-3-acetic Acid (IAA) Production by *Bacillus megaterium* BMS. *Han'guk T'oyang Piryu Hakhoechi* **2016**, *49*, 461–468.
- (24) Napier, R. M.; David, K. M.; Perrot-Rechenmann, C. A short history of auxin-binding proteins. *Plant Mol. Biol.* **2002**, *49* (3–4), 339–48.
- (25) Kramer, J.; Özkaya, Ö.; Kümmerli, R. Bacterial siderophores in community and host interactions. *Nat. Rev. Microbiol.* **2020**, *18* (3), 152–163.
- (26) Mendonca, C. M.; Yoshitake, S.; Wei, H.; Werner, A.; Sasnow, S. S.; Thannhauser, T. W.; Aristilde, L. Hierarchical routing in carbon metabolism favors iron-scavenging strategy in Fe-deficient soil *Pseudomonas* species. *Proc. Natl. Acad. Sci. U. S. A.* **2020**, *117* (51), 32358–32369.
- (27) Mullis, K. B.; Pollack, J. R.; Neilands, J. B. Structure of schizokinen, An iron-transport compound from *Bacillus megaterium*. *Biochemistry* **1971**, *10* (26), 4894–4898.
- (28) Lindsay, W. L.; Schwab, A. P. The chemistry of iron in soils and its availability to plants. *J. Plant Nutr.* **1982**, *5* (4–7), 821–840.
- (29) Keel, C.; et al. Suppression of root diseases by *Pseudomonas fluorescens* CHA0: Importance of the bacterial secondary metabolite 2,4-diacetylphloroglucinol. *Mol. Plant-Microbe Interact.* **1992**, *5*, 4–13.
- (30) Howell, C. R.; Stipanovic, R. D. Suppression of Pythium ultimum-induced damping-off of cotton seedlings by *Pseudomonas fluorescens* and its antibiotic, pyoluteorin. *Phytopathology* **1980**, *70*, 712–715.
- (31) Nowak-Thompson, B.; Chaney, N.; Wing, J. S.; Gould, S. J.; Loper, J. E. Characterization of the pyoluteorin biosynthetic gene cluster of *Pseudomonas fluorescens* Pf-5. *J. Bacteriol.* **1999**, *181* (7), 2166–2174.
- (32) Duke, S. O.; et al. Glyphosate effects on plant mineral nutrition, crop rhizosphere microbiota, and plant disease in glyphosate-resistant crops. *J. Agric. Food Chem.* **2012**, *60* (42), 10375–10397.
- (33) Zobielle, L. H.; Kremer, R. J.; Oliveira, R. S., Jr; Constantin, J. Glyphosate affects micro-organisms in rhizospheres of glyphosate-resistant soybeans. *J. Appl. Microbiol.* **2011**, *110* (1), 118–127.
- (34) Busse, M. D.; Ratcliff, A. W.; Shestak, C. J.; Powers, R. F. Glyphosate toxicity and the effects of long-term vegetation control on soil microbial communities. *Soil Biol. Biochem.* **2001**, *33* (12–13), 1777–1789.
- (35) Pline, W. A.; Lacy, G. H.; Stromberg, V.; Hatzios, K. K. Antibacterial Activity of the Herbicide Glufosinate on *Pseudomonas syringae* Pathovar Glycinea. *Pestic. Biochem. Physiol.* **2001**, *71* (1), 48–55.
- (36) Shushkova, T. V.; Ermakova, I. T.; Sviridov, A. V.; et al. Biodegradation of glyphosate by soil bacteria: Optimization of cultivation and the method for active biomass storage. *Microbiology* **2012**, *81*, 44–50.

- (37) Masotti, F.; Garavaglia, B. S.; Piazza, A.; Burdisso, P.; Altabe, S.; Gottig, N.; Ottado, J. Bacterial isolates from Argentine Pampas and their ability to degrade glyphosate. *Sci. Total Environ.* **2021**, *774*, 145761.
- (38) Hsiao, C.; Young, C.; Wang, C. Screening and identification of glufosinate-degrading bacteria from glufosinate-treated soils. *Weed Sci.* **2007**, *55* (6), 631–637.
- (39) Naylor, R. E. L. *Weed Management Handbook*, 9th ed.; Blackwell Science for British Crop Protection Council: Oxford, 2002.
- (40) Steinrucken, H. C.; Amrhein, N. The herbicide glyphosate is a potent inhibitor of 5-enolpyruvyl shikimate acid-3-phosphate synthase. *Biochem. Biophys. Res. Commun.* **1980**, *94*, 1207–1212.
- (41) Donn, G.; Köcher, H.; Böger, P.; Wakabayashi, K.; Hirai, K. Inhibitors of Glutamine Synthetase. *Herbicide Classes in Dev.: Mode of Action, Targets, Genetic Eng., Chem.* **2002**, 87–101.
- (42) Aristilde, L.; Reed, M. L.; Wilkes, R. A.; Youngster, T.; Kukurugya, M. A.; Katz, V.; Sasaki, C. R. S. Glyphosate-Induced Specific and Widespread Perturbations in the Metabolome of Soil *Pseudomonas* Species. *Front. Environ. Sci.* **2017**, *5*, 34.
- (43) Herrmann, K. M.; Weaver, L. M. The shikimate pathway. *Annu. Rev. Plant Physiol. Plant Mol. Biol.* **1999**, *50* (1), 473–503.
- (44) Somers, E.; Ptacek, D.; Gysegom, P.; Srinivasan, M.; Vanderleyden, J. *Azospirillum brasilense* produces the auxin-like phenylacetic acid by using the key enzyme for indole-3-acetic acid biosynthesis. *Appl. Environ. Microbiol.* **2005**, *71*, 1803–1810.
- (45) Lin, G.; Chang, C. Y.; Lin, H. R. Systematic profiling of indole-3-acetic acid biosynthesis in bacteria using LC-MS/MS. *J. Chromatogr. B: Anal. Technol. Biomed. Life Sci.* **2015**, *988*, 53–28.
- (46) Niessen, N.; Soppa, J. Regulated Iron Siderophore Production of the Halophilic Archaeon *Haloferax volcanii*. *Biomolecules* **2020**, *10* (7), 1072.
- (47) Thiour-Mauprivez, C.; et al. Effects of herbicide on non-target microorganisms: Towards a new class of biomarkers? *Sci. Total Environ.* **2019**, *684*, 314–325.
- (48) Yan, Q.; Philmus, B.; Chang, J. H.; Loper, J. E. Novel mechanism of metabolic co-regulation coordinates the biosynthesis of secondary metabolites in *Pseudomonas protegens*. *eLife* **2017**, *6*, e22835.
- (49) Arentson, B. W.; Sanyal, N.; Becker, D. F. Substrate channeling in proline metabolism. *Front. Biosci., Landmark Ed.* **2012**, *17*, 375–388.
- (50) Shimizu, H.; Hirasawa, T. Production of glutamate and lutamate-related amino acids: molecular mechanism analysis and metabolic engineering. *Microbiol Monogr (5) Amino Acid Biosynth.* **2007**, *5*, 1–38.
- (51) Clarke, S. D.; Nakamura, M. T.; Lennarz, W. J.; Lane, M. D. Fatty Acid Structure and Synthesis. *Encycl. Biol. Chem.* **2013**, 285–289.
- (52) Colombo, C.; et al. Review on iron availability in soil: interaction of Fe minerals, plants, and microbes. *J. Soils Sediments* **2014**, *14* (3), 538–548.
- (53) Mendonca, C. M.; Reed, M. L.; Kukurugya, M. A.; Aristilde, L. Adverse Metabolic Outcomes in Soil *Pseudomonas* Species Exposed to Polyethoxylated Tallow Amine and Glyphosate. *Environ. Sci. Technol. Lett.* **2019**, *6* (8), 448–455.
- (54) Youngster, T.; et al. Profiling glucose-induced selective inhibition of disaccharide catabolism in *Bacillus megaterium* QM B1551 by stable isotope labelling. *Microbiology (London, U. K.)* **2017**, *163* (10), 1509–1514.
- (55) Shehata, A. A.; Schrödl, W.; Aldin, A. A.; Hafez, H. M.; Krüger, M. The effect of glyphosate on potential pathogens and beneficial members of poultry microbiota in vitro. *Curr. Microbiol.* **2013**, *66* (4), 350–358.
- (56) Liu, X.; et al. Development and quantitative evaluation of a high-resolution metabolomics technology. *Anal. Chem.* **2014**, *86* (4), 2175–2184.
- (57) Marek, L. J.; Koskinen, W. C. Simplified analysis of glyphosate and aminomethylphosphonic acid in water, vegetation and soil by liquid chromatography-tandem mass spectrometry. *Pest Manage. Sci.* **2014**, *70* (7), 1158–1164.
- (58) Xie, Y.; et al. A rifampicin-resistant (*rpoB*) mutation in *Pseudomonas protegens* Pf-5 strain leads to improved antifungal activity and elevated production of secondary metabolites. *Res. Microbiol.* **2016**, *167* (8), 625–629.
- (59) Alexander, D. B.; Zuberer, D. A. Use of chrome azurol S reagents to evaluate siderophore production by rhizosphere bacteria. *Biol. Fertil. Soils* **1991**, *12*, 39–45.
- (60) Carpio, M. J. Soil Microbial Community Changes in a Field Treatment with Chlorotoluron, Flufenacet and Diflufenican and Two Organic Amendments. *Agronomy* **2020**, *10* (8), 1166.
- (61) Murínová, S.; Dercová, K. Response Mechanisms of Bacterial Degraders to Environmental Contaminants on the Level of Cell Walls and Cytoplasmic Membrane. *Int. J. Microbiol.* **2014**, *2014*, 873081.
- (62) Uniprot Consortium. UniProt: the universal protein knowledgebase in 2021. *Nucleic Acids Res.* **2020**, *49* (D1), D480–D489.
- (63) Schönbrunn, E.; et al. Interaction of the herbicide glyphosate with its target enzyme 5-enolpyruvylshikimate 3-phosphate synthase in atomic detail. *Proc. Natl. Acad. Sci. U. S. A.* **2001**, *98* (4), 1376–1380.
- (64) Ahemad, M.; Khan, M. S. Toxicological Effects of Selective Herbicides on Plant Growth Promoting Activities of Phosphate Solubilizing *Klebsiella* sp. Strain PS19. *Curr. Microbiol.* **2011**, *62* (2), 532–538.
- (65) Staub, J. M.; Brand, L.; Tran, M.; Kong, Y.; Rogers, S. G. Bacterial glyphosate resistance conferred by overexpression of an *E. coli* membrane efflux transporter. *J. Ind. Microbiol. Biotechnol.* **2012**, *39* (4), 641–647.
- (66) Kumar, V.; Singh, S.; Upadhyay, N. Effects of organophosphate pesticides on siderophore producing soil microorganisms. *Biocatal. Agric. Biotechnol.* **2019**, *21*, 101359.
- (67) Brodhagen, M.; et al. Reciprocal regulation of pyoluteorin production with membrane transporter gene expression in *Pseudomonas fluorescens* Pf-5. *Appl. Environ. Microbiol.* **2005**, *71* (11), 6900–6909.
- (68) Brodhagen, M.; et al. Positive autoregulation and signaling properties of pyoluteorin, an antibiotic produced by the biological control organism *Pseudomonas fluorescens* Pf-5. *Appl. Environ. Microbiol.* **2004**, *70* (3), 1758–1766.
- (69) Schnider-Keel, U.; et al. Autoinduction of 2,4-diacetylphloroglucinol biosynthesis in the biocontrol agent *Pseudomonas fluorescens* CHA0 and repression by the bacterial metabolites salicylate and pyoluteorin. *J. Bacteriol.* **2000**, *182* (5), 1215–1225.
- (70) Tian, T.; et al. The resistance-nodulation-division efflux pump EmhABC influences the production of 2,4-diacetylphloroglucinol in *Pseudomonas fluorescens* 2P24. *Microbiology (London, U. K.)* **2010**, *156* (1), 39–48.
- (71) Lim, C. K.; et al. The effect of iron limitation on the transcriptome and proteome of *Pseudomonas fluorescens* Pf-5. *PLoS One* **2012**, *7* (6), e39139.
- (72) Morillo, E.; et al. Glyphosate adsorption on soils of different characteristics.: Influence of copper addition. *Chemosphere* **2000**, *40* (1), 103–107.
- (73) Pereira, R. C.; et al. The effect of pH and ionic strength on the adsorption of glyphosate onto ferrihydrite. *Geochem. Trans.* **2019**, *20* (1), 3.
- (74) Gimsing, A. L.; Borggaard, O. K. Competitive adsorption and desorption of glyphosate and phosphate on clay silicates and oxides. *Clay Miner.* **2002**, *37* (3), 509–515.
- (75) Maqueda, C.; et al. Behaviour of glyphosate in a reservoir and the surrounding agricultural soils. *Sci. Total Environ.* **2017**, *593*–594, 787–795.
- (76) Ololade, I. A.; et al. Sorption of Glyphosate on Soil Components: The Roles of Metal Oxides and Organic Materials. *Soil Sediment Contam.* **2014**, *23* (5), 571–585.
- (77) Khenifi, A.; Derriche, Z.; Mousty, C.; Prevot, V.; Forano, C. Adsorption of Glyphosate and Glufosinate by Ni₂Al₂O₃ layered double hydroxide. *Appl. Clay Sci.* **2010**, *47*, 362–371.

- (78) Khoury, G. A.; et al. Glyphosate adsorption on montmorillonite: An experimental and theoretical study of surface complexes. *Appl. Clay Sci.* **2010**, *50* (2), 167–175.
- (79) Xu, J.; et al. Adsorption behavior and mechanism of glufosinate onto goethite. *Sci. Total Environ.* **2016**, *560–561*, 123–130.
- (80) Khenifi, A.; et al. Adsorption of glyphosate and glufosinate by Ni₂AlNO₃ layered double hydroxide. *Appl. Clay Sci.* **2010**, *47* (3–4), 362–371.
- (81) Ghassemi, M.; et al. Environmental effects of new herbicides for vegetation control in forestry. *Environ. Int.* **1982**, *7* (6), 389–401.